

Seismic Performance Evaluation of Tall Buildings with Axi-symmetric Plans

Joonho Lee and Jieun Kong

Graduate Student, Department of Architectural Engineering, Sungkyunkwan University, Suwon, Korea

Jinkoo Kim

Corresponding Author, Professor, Department of Architectural Engineering, Sungkyunkwan University, Suwon, Korea



SUMMARY:

In this study the seismic performance of axi-symmetric tall building structures are evaluated by nonlinear static and dynamic analyses. For analysis models, thirty three-story convex, concave, and gourd-type axi-symmetric buildings are designed to have similar floor areas using diagrid structure system, and their performances are compared with that of a regular moment frame building. The stiffness and strength of each system are obtained by nonlinear static analysis and incremental dynamic analysis. Seismic fragility analyses are carried out using forty four earthquake records to compare the probability of failure for a given earthquake intensity. The validity of the seismic performance factor used for design of the model structures is evaluated based on the procedure recommended in the ATC-63 report. Based on the analysis results, the effect of variation in the overall shape of axi-symmetric tall buildings on the seismic performance is evaluated.

Keywords : ATC-63, axi-symmetric buildings, tall buildings, seismic performance factor

1. INTRODUCTION

Recently the geometric complexity and irregularity of building structures have been rapidly increasing, which significantly affects the seismic performance of the structures. Vollers (2008) proposed a morphological scheme which enables data to be retrieved on sustainable performance of building shapes. He categorized the geometry of high-rise buildings into *Extruders*, *Rotors*, *Twisters*, *Tordos*, *Transformers*, and *Free Shapers* depending on their form-generation method. In this study the seismic performance of the Rotor-type or axi-symmetric tall building structures was evaluated by nonlinear static and dynamic analyses. For analysis models, thirty three-story convex, concave, and gourd-type axi-symmetric buildings are designed to have similar floor areas using diagrid structure system, and their performances are compared with that of a regular moment frame building. The stiffness and strength of each system were obtained by nonlinear static and incremental dynamic analyses. The validity of the seismic performance factor used for seismic design was evaluated following the procedure recommended in the ATC-63 (2009) report. Seismic fragility analyses were carried out using forty earthquake records to compare the probability of failure for a given earthquake intensity. Based on the analysis results, the effect of variation in the overall shape of axi-symmetric tall buildings on the seismic performance was also evaluated.

2. SEISMIC PERFORMANCE EVALUATION PROCEDURE OF ATC-63

The ATC-63 recommended a methodology for quantifying building system performance and response parameters for use in seismic design. the methodology achieves the primary life safety performance objective by requiring an acceptably low probability of collapse of the seismic-force resisting system

when subjected to maximum considered earthquake (MCE) ground motions. the methodology consists of a framework for establishing seismic performance factors (SPFs) that involves development of detailed system design information and probabilistic assessment of collapse risk. it utilizes nonlinear analysis techniques, and explicitly considers uncertainties in ground motion, modelling, design, and test data. the technical approach is a combination of traditional code concepts, advanced nonlinear dynamic analyses, and risk-based assessment techniques.

In ATC-63 collapse assessment is performed using nonlinear static (pushover) and nonlinear dynamic (response history) analysis procedures. Nonlinear static analyses are used to help validate the behavior of nonlinear models and to provide statistical data on system overstrength and ductility capacity. Nonlinear dynamic analyses are used to assess median collapse capacities, and collapse margin ratios. Nonlinear response is evaluated for a set of pre-defined ground motions which include twenty-two ground motion record pairs from sites located greater than or equal to 10 km from fault rupture, referred to as the “Far-Field” record set. The ground motions are collectively scaled (or “anchored”) to a specific ground motion intensity such that the median spectral acceleration of the record set matches spectral acceleration at the fundamental period of the structure being analyzed. This scaling process parallels the ground motion scaling requirements of ASCE/SEI 7-05.

Nonlinear dynamic analyses are conducted to establish the median collapse capacity, \widehat{S}_{CT} , and collapse margin ratio (*CMR*) for each of the analysis models. The ratio between the median collapse intensity and the MCE intensity is defined as the collapse margin ratio (*CMR*), which is the primary parameter used to characterize the collapse safety of the structure.

$$CMR = \frac{\widehat{S}_{CT}}{S_{MT}} = \frac{SD_{CT}}{SD_{MT}} \quad (1)$$

To account for the effect of spectral shape in determination of the collapse margin ratio, the spectral shape factors, *SSF*, which depend on fundamental period, *T*, and ductility capacity, μ_c , are used to adjust collapse margin ratios. The adjusted collapse margin ratio (*ACMR*) is obtained by multiplying tabulated *SSF* values with the collapse margin ratio that was predicted using the Far-Field record set.

Acceptable values of adjusted collapse margin ratio are based on total system collapse uncertainty, β_{TOT} , and established values of acceptable probabilities of collapse. They are based on the assumption that the distribution of collapse level spectral intensities is lognormal, with a median value, \widehat{S}_{CT} , and a lognormal standard deviation equal to the total system collapse uncertainty, β_{TOT} .

$$\beta_{TOT} = \sqrt{\beta_{RTR}^2 + \beta_{DR}^2 + \beta_{TD}^2 + \beta_{MDL}^2} \quad (2)$$

The total system collapse uncertainty is a function of record-to-record (RTR) uncertainty, design requirements related (DR) uncertainty, test data-related (TD) uncertainty, and modeling (MDL) uncertainty. Quality ratings for design requirements, test data, and nonlinear modeling are translated into quantitative values of uncertainty based on the following scale: (A) Superior, $\beta = 0.20$; (B) Good, $\beta = 0.30$; (C) Fair, $\beta = 0.45$; and (D) Poor, $\beta = 0.65$. Values of total system collapse uncertainty, β_{TOT} , are provided in Table 7-2 of the ATC-63. Table 7-3 of the ATC-63 and Table 3 of this paper provides acceptable values of adjusted collapse margin ratio, *ACMR10%* and *ACMR20%*, based on total system collapse uncertainty and values of acceptable collapse probability, taken as 10% and 20%, respectively.

3. DESIGN AND ANALYSIS MODELING OF MODEL STRUCTURES

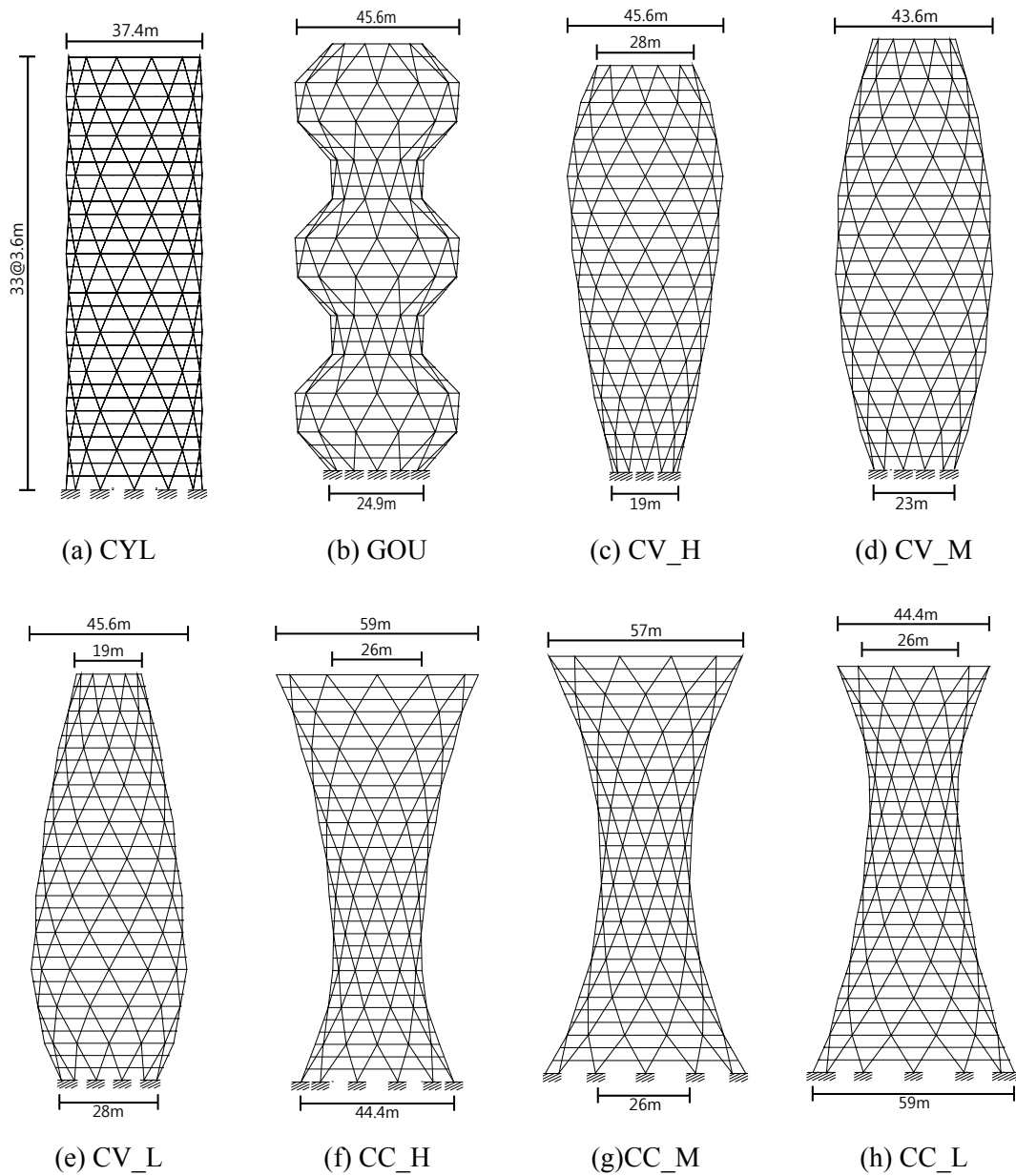


Fig. 1 Elevation of 33-story analysis model structures

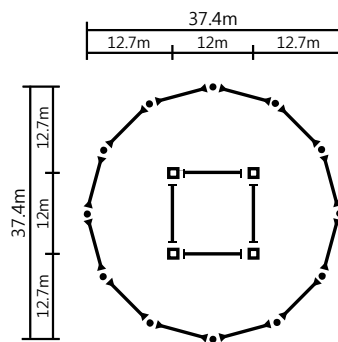


Fig. 2 Floor plan of the cylinder type case study buildings

The analysis model structures are 33-story diagrid structures with the cylindrical, convex, concave, and the gourd shapes as shown in Fig. 1. To compare the seismic performances, the model structures were designed to have similar total floor area. Fig. 2 depicts the structural plan shape of the cylinder type structure. The perimeter beams were designed with H-shaped rolled sections with ultimate strength of 400 N/mm^2 , and the core columns were designed with box shape steel with ultimate strength of 490 N/mm^2 . The diagrid members were designed with circular hollow steel sections with ultimate strength of 490 N/mm^2 . The floor slabs were considered as rigid diaphragm. The model structures were designed with the dead and live loads of 6kN/m^2 and 2.5kN/m^2 , respectively, and wind load with basic wind speed of 30m/sec . The seismic load was evaluated based on the spectral acceleration coefficients of $S_{DS}=0.43$ and $S_{D1}=0.23$ with the response modification factor of 3.0 in the ASCE 7-10 (2010) format. The structural design was carried out using the structural analysis/design program code MIDAS (MIDASIT 2009) based on the AISC LRFD Specifications. Table 2 shows the total floor areas and fundamental periods of the model structures, and Table 3 shows the design base shears and steel tonnages of the model structures. It can be observed that the natural period is larger in the model structures with their center of mass located at higher levels. The convex type structures have larger period than concave type structures. The natural period of the gourd type structure is longer than twice that of the cylinder type structure. The number in the parenthesis represents the ratio of the steel tonnage of the structure and that of the cylinder type structure. It can be observed that the smallest amount of structural steel was used in the design of cylinder type structure, and the largest steel was used in the gourd type structure.

For nonlinear analysis of bending members the skeleton curve provided in the FEMA-356 (2000) and shown in Fig. 3(a) was used. The parameters a , b , and c vary depending on the width-thickness ratio of the structural members, and were determined based on the guidelines provided in the Tables 5-6 and 5-7 of the FEMA-356. The post-yield stiffness of 3% was generally used for modeling of bending members. For nonlinear analysis of bracing members, the generalized load-deformation curves recommended in the FEMA-274 (1997) and shown in Fig. 3(b) were used.

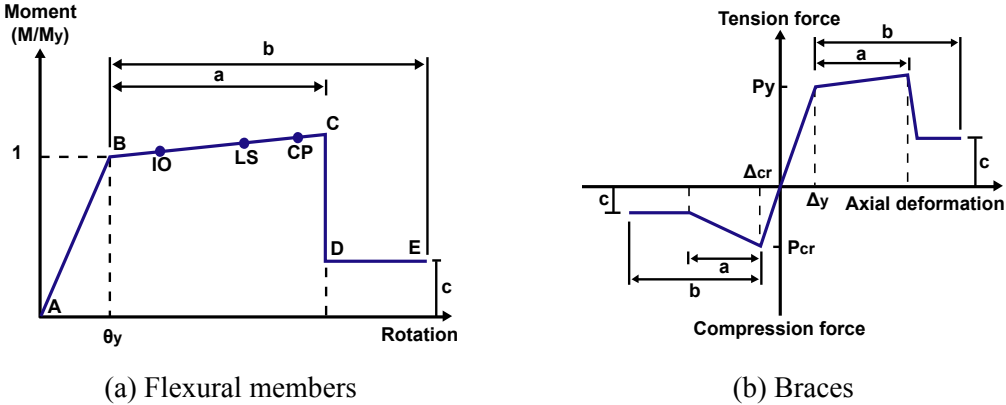


Fig. 3 Nonlinear force-deformation relationships for structural members

4. APPLICATION OF ATC-63 PROCEDURE

The 44 ground motions presented in the ATC-63 were collectively scaled in such a way that the median spectral acceleration of the record set matches the MCE design spectral acceleration at the fundamental period of the model structures. Plots of the response spectra for the record set, and an illustration of intensity anchoring to the MCE design spectrum corresponding to the fundamental natural period of the cylinder-type model structure, are shown in Fig. 4.

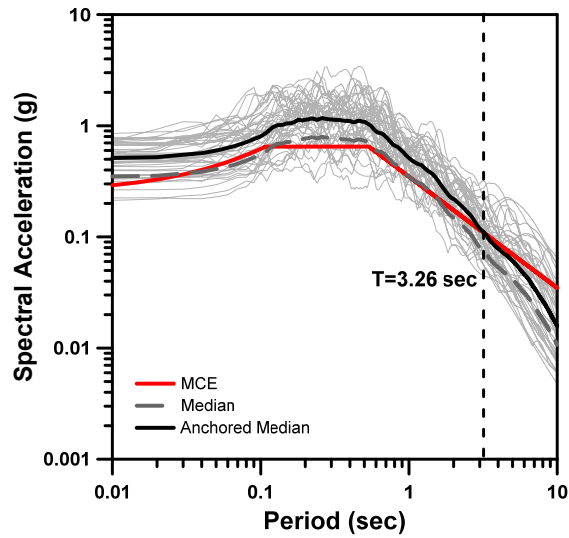
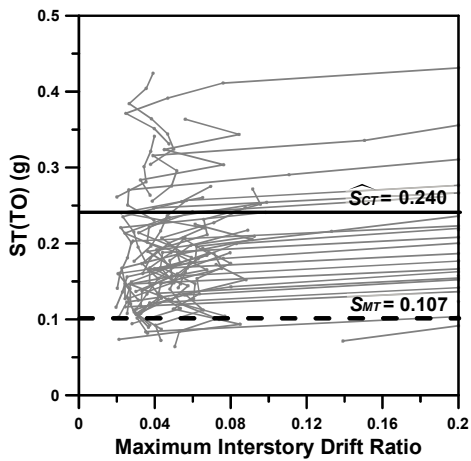
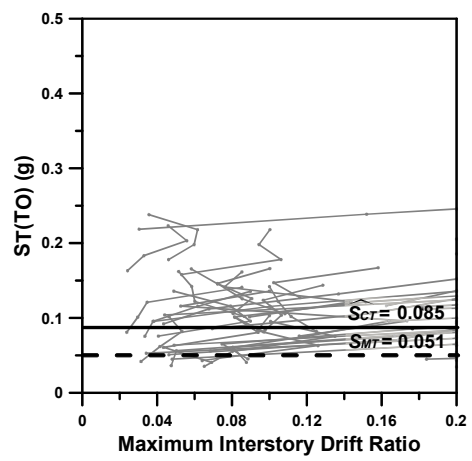


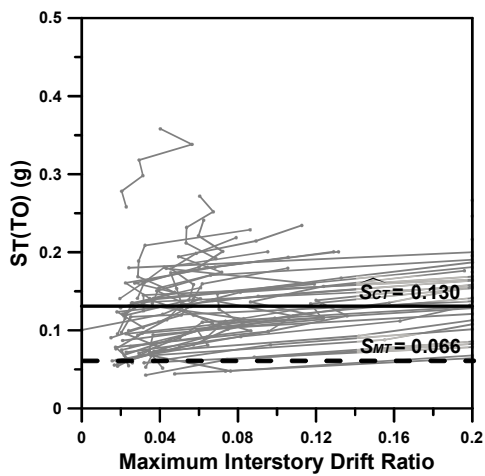
Fig. 4 Response spectra for the record set and intensity anchoring to the MCE design spectrum corresponding to the fundamental natural period of the cylinder-type model structure



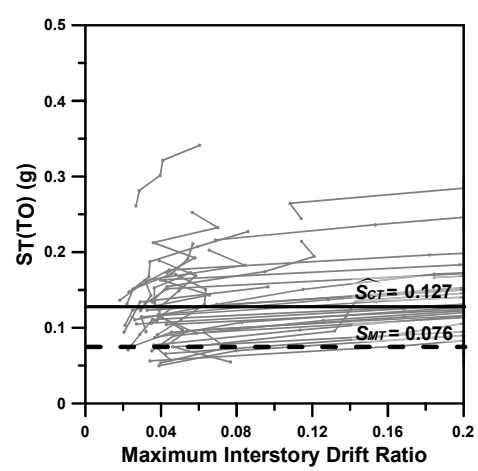
(a) CYL



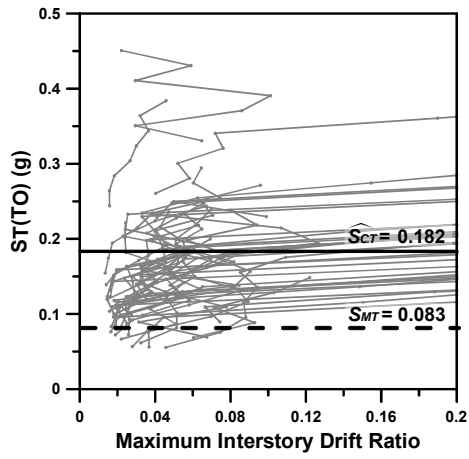
(b) GOU



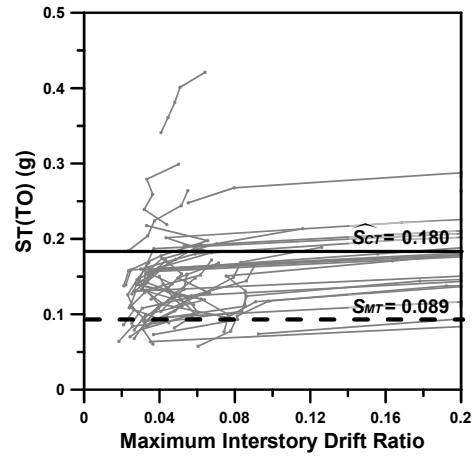
(c) CV_H



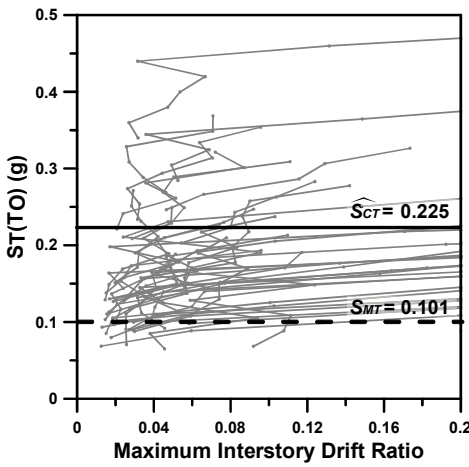
(d) CC_H



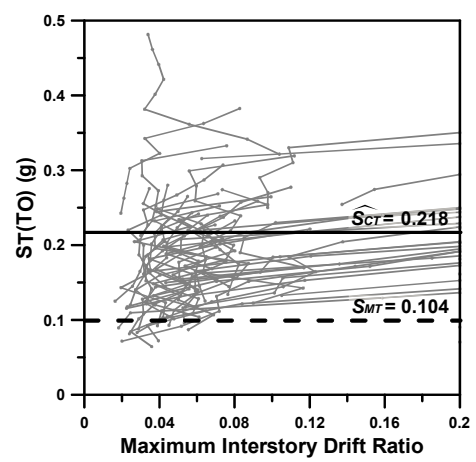
(e) CV_M



(f) CC_M



(g) CV_L



(h) CC_L

Fig. 5 Determination of $\bar{\mu}_{2/22}$ from incremental dynamic analyses

Table 1. Collapse margin ratios of the model structures

Type		$\bar{\mu}_{2/22}$	CMR
CYL	0.107	0.240	2.243
GOU	0.051	0.085	1.667
CV_H	0.066	0.130	1.970
CV_M	0.083	0.182	2.193
CV_L	0.101	0.225	2.228
CC_H	0.076	0.127	1.671
CC_M	0.089	0.180	2.022
CC_L	0.104	0.218	2.096

Collapse is judged to occur from dynamic instability at which excessive displacement occurs without increase in spectral acceleration. Incremental dynamic analyses were carried out increasing the intensity of the records by 0.02g until dynamic instability occurred for 22 earthquake records. Fig. 5 shows the IDA curves of the model structures including such information as the MCE spectral acceleration, S_{MT} , and the median collapse capacity, \widehat{S}_{CT} . Those information are summarized in Table 1 along with the collapse margin ratio (CMR) for all model structures. It can be observed that the cylinder-type structure has the largest margin for collapse followed by the concave-type structure with low center of mass. The CMR of the gourd-type structure and the concave structure with high center of mass (model CC_H) are the smallest. As the natural period increases and as the location of the center of mass increases, the MCE spectral acceleration, the median capacity, and the CMR tend to decrease. The collapse margins for concave-type structures turned out to be generally higher than those of the convex-type structures.

Table 2. Adjusted collapse margin ratios of the model structures

Type	T_n	SSF	ACMR
CYL	1.249	1.072	2.404
GOU	1.394	1.094	1.824
CV_H	1.369	1.090	2.147
CV_M	1.323	1.083	2.375
CV_L	1.311	1.082	2.411
CC_H	1.271	1.076	1.798
CC_M	1.227	1.069	2.161
CC_L	1.253	1.073	2.249

Table 2 shows the period based ductility factors and the spectral shape factors of the model structures obtained from linear interpolation of the SSF presented in Table 7-1 of the ATC-63. Also shown are the ACMR of the model structures obtained by multiplying the SSF with the CMR. Even though the gourd-type model has the smallest CMR, the adjusted value, ACMR, is the smallest in the CC_H structure. Table 7-3 of ATC-63 provides acceptable values of adjusted collapse margin ratio, $ACMR10\%$ and $ACMR20\%$, based on total system collapse uncertainty and values of acceptable collapse probability, taken as 10% and 20%, respectively. Lower values of acceptable collapse probability and higher levels of collapse uncertainty result in higher required values of adjusted collapse margin ratio. Acceptable performance is achieved when individual values of adjusted collapse margin ratio for each structure exceeds $ACMR20\%$. As diagrid structure systems are relatively newly developed and there are no seismic performance factors recommended yet in the design codes, the quality rating for the design requirements was considered to be (C) Fair ($\beta_{DR} = 0.35$). The rating for the test data-related uncertainty was assumed to be (B) Good ($\beta_{TD} = 0.2$), and the modeling uncertainty was also assumed to be (B) Good ($\beta_{MDL} = 0.2$). The uncertainty due to record-to-record variability is recommended to be $\beta_{RTR} = 0.40$ in every case in the ATC-63. The total system collapse uncertainty for the analysis model structures was calculated to be 0.602 using Eq. 2. From Table 7-3 of the ATC-63, the collapse probability of the model structures are obtained as $ACRM 20\% = 1.66$, which is smaller than the ACMR of the model structures. Based on this result, it can be concluded that the seismic performance factors, especially the response modification factor, seem to be appropriate for the seismic design of the analysis model structures.

5. CONCLUSIONS

In this study the seismic performances of axi-symmetric tall building structures were evaluated based on the procedure recommended in the ATC-63. Seismic fragility analyses were carried out using twenty two pairs of earthquake records to compare the probability of failure for a given earthquake intensity. The adjusted collapse margin ratios of the model structures, which were computed using the incremental dynamic analysis of twenty two pairs of ground motions, turned out to be higher than the acceptable values specified in the ATC-63. This implies that the response modification factor of 3.0 used in the design of the model structures is acceptable for the ATC-63 methodology. The margin ratios of the cylinder-type and the convex-type structures were larger than those of the other structures.

AKNOWLEDGEMENT

This work (No. 2011-0015734) was supported by Mid-career Researcher Program through National Research Foundation grant funded by the Korea Ministry of Education, Science and Technology.

REFERENCES

- ATC, Quantification of building seismic performance factors, ATC-63, Applied Technology Council, Redwood City, CA., 2009
- ASCE (2005), Minimum Design Loads for Buildings and Other Structures, ASCE 7-05, American Society of Civil Engineers.
- Computers and Structures, Inc. (2006), PERFORM Components and Elements for PERFORM 3D and PERFORM-Collapse Version 4, CSI, Berkeley, CA.
- FEMA (2000), Prestandard and commentary for the seismic rehabilitation of buildings, FEMA-356, Federal Emergency Management Agency, Washington, D.C.
- FEMA, NEHRP Recommended Provisions for Seismic Regulations for New Buildings and Other Structures, FEMA 450, Federal Emergency Management Agency, Washington, D.C., 2003
- ICC (2006), International Code Council, International Building Code, Falls Church, Virginia.
- MIDAS (2009), General Structure Design System for Window, Ver. 7.7.0.
- Vollers, K., Morphological scheme of second-generation non-orthogonal high-rises, CTBUH 8th World Congress 2008